Extended LHCD Capability towards Steady-State Plasma in EAST

B J Ding, F K Liu, J G Li and B N Wan **for LHCD group, EAST team and collaborators**

Institute of Plasma Physics, Chinese Academy of Sciences, Hefei 230031, P. R. China

Email: bjding@ipp.ac.cn

Abstract In addition to 2.45GHz/4MW lower hybrid current drive (LHCD) system, a 4.6GHz LHCD system has been firstly commissioned in EAST in 2014 campaign. First LHCD results with 4.6GHz show that LHW can be coupled to plasma with low reflection coefficient, drive plasma current, modify plasma current profile, and heat plasma effectively. Also, CD efficiency and current profile depend on the launched wave spectrum, suggesting the possibility of controlling current profile by changing phase difference. Repeatable H-mode plasma is obtained by either 4.6GHz LHCD system alone, or together with the 2.45GHz LHCD system, the NBI (neutral beam injection) system.

1. Introduction

Lower hybrid current drive (LHCD) [1–3] plays a key role in controlling current profile in tokamak experiments aimed at achieving important goals relevant to fusion plasma. For steady-state plasma with LHCD in EAST [4], high LH power is necessary. Also, at high density, LH wave with higher frequency is preferred so as to avoid the interaction between LH wave and ions. To obtain EAST scientific goal (long pulse and high performance), a new LHCD system (4.6GHz/6MW, CW), which consists of 24 klystrons, has been installed in EAST and commissioned in 2014. Up to now, together with 2.45GHz/4MW LHCD system, the total available LHCD power is up to 10MW in EAST. For the 2.45GHz system, many LHCD results have been reported[5, 6-11], including coupling and current drive at different conditions.

In this paper, the preliminary experimental results with 4.6GHz system and some investigations are presented, in which the toroidal magnetic field (B_t) is about 2.3T.The working gas is with deuterium (D_2) and usual configuration mentioned in this paper is lower single null (LSN).

2. Description of 4.6GHz LHCD system

In EAST, the 4.6GHz LHCD system consists of power supply, klystrons (total 24), transmission line (circulator, directional coupler, ceramic windows, waveguide, etc), and antenna. LHW from micro-wave source to transmission line is launched into the tokamak plasma by a multi-junction grill [12, 13] type of antenna with 24 modules arranged in an array of 4 rows and 6 columns. Each module (main waveguide), supplied by one power system, is divided into 3 sub-rows in poloidal direction and, in each sub-row, consists of 8 active sub-waveguides between which there is a 90^0 phase difference generated by a built-in phase shifter, which is composed of quarter wavelength step transformers and a straight waveguide with reduced height. In each sub-row of the launcher, there are 7 passive waveguides inserted between the adjacent

main waveguides. Therefore, the whole launcher is composed of 660 sub-waveguides (576 active and 84 passive sub-waveguides). The height and the width of each sub-waveguide are 5cm and 0.6 cm for wave propagation, respectively. The system is cooled by water during the operation. The calculated power spectrum by a linear coupling code ALOHA [14] is displayed in Fig.1, where $N_{//}^{peak}$ is the peak index of parallel refraction of the launched wave. The power spectrum of launched waves can be adjusted by changing the phase difference ($\Delta\Phi$) between the adjacent main waveguides from -180^0 to 180^0.

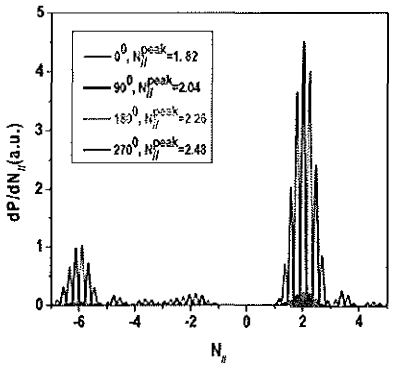

Fig. 1 Power spectrum (4.6GHz antenna) calculated by ALOHA code

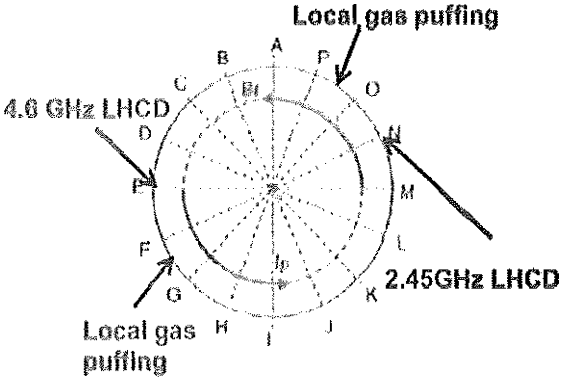

Fig. 2 Top view of ports of local gas puffing and LHCD antenna (the directions of Ip and Bt are indicated)

3. LHW-plasma coupling experiments

In EAST, LHW antenna with 4.6 GHz and 2.45GHz are installed in E port and N port (see Fig. 2), respectively. In order to improve LHW–plasma coupling for 2.45GHz and 4.6GHz LHW as shown in Fig. 2, two local gas pipes covering the whole grill in the poloidal direction have been installed at the electron-drift side of the LHW antenna for the new campaign, between the port of O and P port, and F and G port in EAST, respectively. The layout of the top view is shown in Fig.2, in which the direction of plasma current (Ip) and toroidal magnetic field (Bt) are also shown. The major radius of the pipe location is about 2400 mm and the radial position of LH antenna is about 2355mm in routine experiments.

First of all, the coupling experiments with and without local gas puffing with the typical phase difference of 90^0 between the main waveguides are performed in EAST. Coupling characteristics by means of the reflection coefficient (RC) and grill density measurements are shown in Fig. 3, where the grill density (n_{e_grill}) is measured by a Langmuir probe installed on the top of the LH antenna, and cut-off density (n_{e_co}) is also plotted. It is shown that with a grill density larger than the cut-off density, RC is relative low (~6%), whereas RC increases quickly when the density is below the cut-off value. The reflection coefficient without local gas putting is higher than that with local gas puffing, implying that the good coupling is obtained by the local gas puffing. The coupling characteristics between L-mode and H-mode are also compared in Fig. 4, showing that, though the RC in H-mode is higher than that in L-mode, its level remains acceptable and does not much affect the coupling.

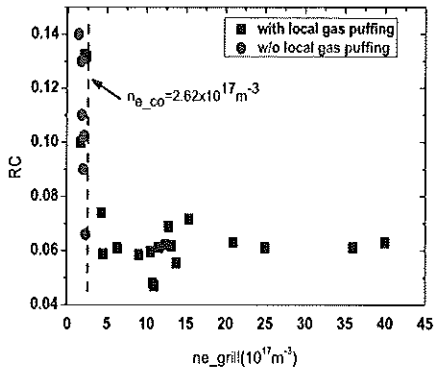

Fig. 3 Coupling characteristics of 4.6GHz LH antenna with/without local gas puffing

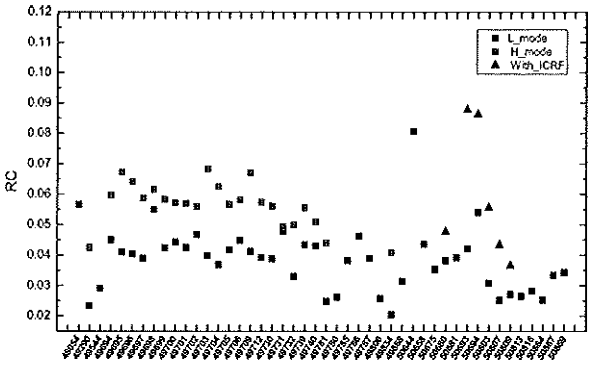

Fig. 4 Coupling characteristics comparison between L-mode and H-mode

Typical waveform (with phase difference of 90^0) including coupling and current drive are shown in Fig.5, indicating that good coupling is obtained by means of local gas puffing and configuration optimization. The maximum power of coupled to plasma is up to 3.5MW in this campaign, suggesting that by means of configuration optimization and local gas puffing, LHW can be effectively coupled into plasma with the present system.

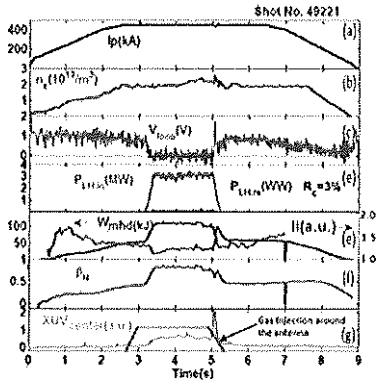

Fig. 5 Typical waveform of coupling, current drive and plasma heating

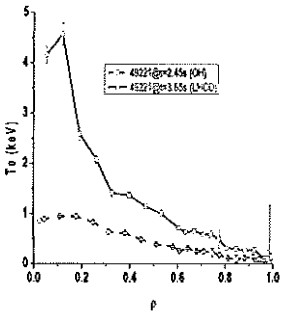

Fig. 6 Te profile measured with Thomson scattering system

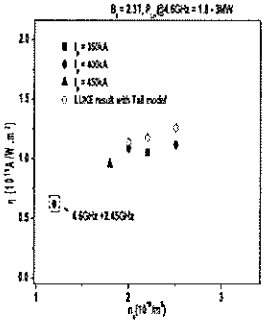

Fig. 7 Experimental and simulated CD efficiency with 4.6GHz LHCD system

4. Experiments of current drive and plasma heating

As shown in Fig.5, the loop voltage decreases quickly to zero approximately, meaning that LHW can drive plasma current effectively. Also, the energy increase from 50kJ to 100kJ and normalized beta increases from 0.4 to 0.8 due to LHCD, suggesting that LH power is effectively coupled to plasma and fully transferred plasma. In addition, the internal inductance (li) decreases after LHCD is applied compared to Ohmic plasma, implying the plasma current profile is broadened by the application of the LH wave.

The electron temperature profile measured by Thomson scattering (TS) [15] is plotted in Fig.6.As compared to the Ohmic plasma, the electron temperature increases much during the LHCD phase and the temperature in core region increases from 1.0keV to

4.5keV, suggesting that plasma is effectively heated by LHW by mean of slowing down of fast electrons and that LHW is mainly deposited in core region.

In the experiments, fully driven current plasma is obtained with different plasma current, which is very convenient to investigate the CD efficiency since we do not need to consider the effect of the Ohmic electric field. Assuming the absorption efficiency of LHW power is 75%, the estimated CD efficiency is shown in Fig. 7. It shows that the CD efficiency is up to $1.1\times10^{19}Am^{-2}W^{-1}$,which is a little higher than that of 2.45GHz LHW [7]. The experimental CD efficiency is weakly evolving with the electron density, which is consistent with the calculated estimate from C3PO/LUKE code shown in Fig. 7 [16]. In the simulation, the experimental parameters and tail model [17] referring to considering broadened spectrum are used.

5. Effect of power spectrum on current drive

To explore long pulse and high performance with LHCD, high current drive efficiency and the capability of controlling current profile are necessary. The related experiments are carried out with toroidal different phase difference ($\Delta\varphi=0^0$, 90^0, 180^0, -90^0) between the main waveguides in EAST, and correspondingly the calculated launched wave spectrum was shown in Fig.1. The target plasmas and plasma configurations, which are kept the same, were displayed in Fig. 8, in which Ip, the distance between the two magnetic surfaces passing through the upper X-point and the lower X-point in the mid-plane in low field side (Drsep), n_e, P_{LH_in}, and $P_{LH_re}$are plotted from (a) to (e). In the experiments, Drsep>0, =0, and <0 means upper single null (USN), double null (DN) and lower single null (LSN), respectively.

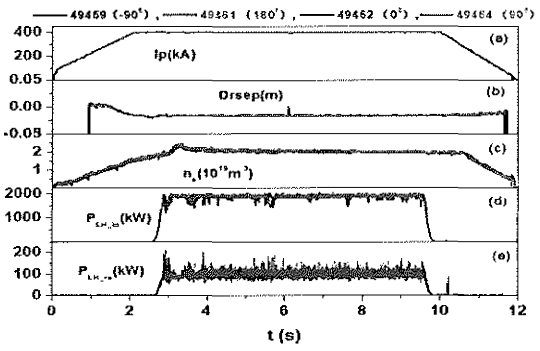

Fig. 8 Target plasmas for effect of power spectrum on current drive

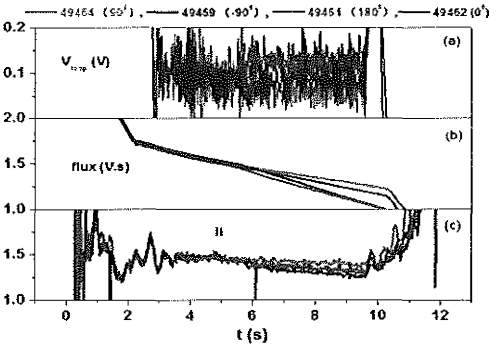

Fig. 9 Effect of spectrum on CD efficiency and current profile

Loop voltages and consumptions of magnetic flux (flux) plotted in Figs. 9 (a) and (b), are the key parameters to investigate the effect of spectrum on CD efficiency, since the total plasma current is feedback controlled by the Ohmic heating power. As shown from Fig.9, though the differences between the various phasings are rather small, the loop voltage is the lowest with $\Delta\varphi=90^0$, which is consistent with the smallest consumptions of magnetic flux, suggesting the highest CD efficiency in this case. The internal inductance is shown in Fig. 9 (c). The value of li is the largest with $\Delta\varphi=90^0$, whereas it is the lowest for $\Delta\varphi=-90^0$, implying the most peaked current density profile with $\Delta\varphi=90^0$.

Note that present differences in loop voltage, consumptions of magnetic flux and li between the cases are not obvious, possibly because the temperature of target plasma is a little low. This could be improved by means of increasing electron temperature, hence enhancing the single pass absorption efficiency. Anyway, above results that current profiles are different with different $\Delta\varphi$ indicates the possibility of profile control by change the wave spectrum as shown in previous LH experiments in many tokamaks [18-23]. Further experiments will be continued with hotter target plasma, e.g., preheated with 2.45GHz LHW, ECRH (electron cyclotron resonance heating), or NBI (neutral beam injection).

6. H-mode plasma with LHCD

To obtain long pulse and high performance plasma, various heating systems are used in EAST, including LHCD, NBI and ion cyclotron radio frequency (ICRF). Based on the above experiments, repeatable H-mode plasmas [24] are obtained by either 4.6GHz LHCD system alone, or together with 2.45GHz LHCD system, NBI system or ICRF system.

Firstly, with the injected LH power of 2.8MW, the longest H-mode plasma with grassy (very small or free) edge localized mode (ELM) up to 28s obtained by 4.6GHz LHCD system alone is shown in Fig. 10, in which Ip, n_e and V_{loop}, P_{LH_in} and P_{LH_re}, W_{mhd} and β_N, and D_a are plotted in (a)-(e). It is observed that the loop voltage remains close to zero, stored energy increases to 130kJ, and the normalized beta is about 1.2. From the statistics of the discharges using the LH system at 4.6GHz shown in Fig. 11, the threshold power for L-H transition is about 1MW in the experiments, which is comparable with the H-mode plasmas obtained with the LH system at 2.45GHz[10]. Further comparison between them will be investigated with a same experimental condition later. The lossed power defined as $P_{loss}= P_{LH} + P_{OH} - P_{rad}$ (P_{LH}, P_{OH}, and P_{rad} are the coupled LH power, Ohmic power and radiation power, respectively)roughly evolves as the scaling law $P_{th}=0.042n_{20}^{0.73}B_t^{0.74}S^{0.98}$ (MW)[25],where S is the plasma surface area in m^2. The operating window for the H-mode is very narrow, the operation space was not varied very much during the experiments, which is to be extended later.

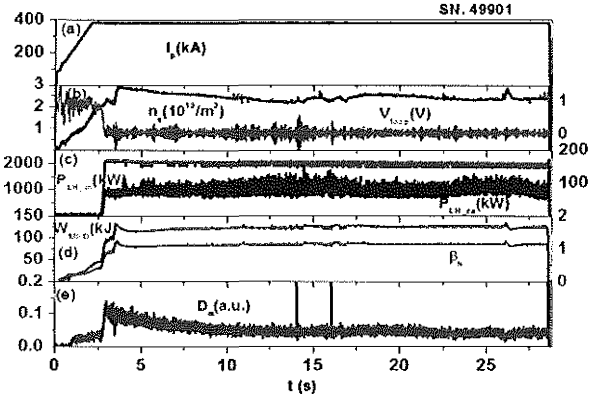

Fig. 10 Typical wave form of H-mode plasma with 4.6GHz LHCD system

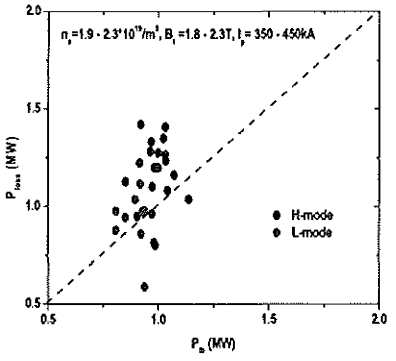

Fig. 11 Threshold power for L-H transition with 4.6GHz LHCD system

Secondly, H-mode is obtained by the LHCD combination of 2.45GHz and 4.6GHz, which is shown in Fig. 12, in which Ip and electron temperature in central region (T_{e0}) measured by Soft X-ray spectrum , n_e and V_{loop}, P_{LH_in}, P_{LH_re}, W_{mhd}, β_N, local gas puffing, and D_a are plotted from (a) to (h), as well as the L-H transition. The H-mode plasma is not observed with the 2.45GHz LH wave alone. A possible explanation is that the LH power injected by this system has not reached the L-H transition threshold. After the application of the LH power at 4.6GHz, the loop voltage decreases somewhat, possibly due to the temperature increase and the additional driven current by LH wave at 4.6GHz. Also, , the electron temperature in core region, the stored energy and normalized beta continue increase after the LH wave application, and then the transition of L-H occurs, indicated the sharp increase in electron density, stored energy and normalized beta, and the sharp decrease in D_a The normalized beta increases from 0.5 to about 1. Around the L-H transition, there is another sharp decrease in loop voltage implying that non-inductive current increases in the H-mode phase, even if the density ($\sim 3.7\times10^{19}m^{-3}$) is much higher than that ($\sim 2.7\times10^{19}m^{-3}$) in the L-mode. This may come from three effects. One is the increase in temperature, which cannot be identified at present due to the time resolution of temperature measurement is not enough. The second is the bootstrap current, which is enhanced due to the pedestal structure. The third is the enhanced CD efficiency, which could be improved by the increased temperature in the edge region due to the pedestal formation. As reported in Ref. 26, high edge temperature may reduce parametric instability behaviour, hence making more waves propagate to core region and enhance CD efficiency. Similar results that higher CD efficiency in H-mode with 2.45GHz LHCD system in EAST have been reported in Refs. 5 and 11. Therefore, high temperature in edge region is expected to improve CD efficiency at high density, e.g., lithium coating or local heating by ECRH in edge region.

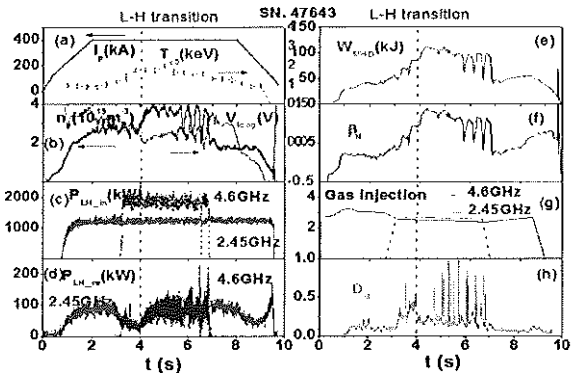

Fig. 12 Typical H-mode with 4.6GHz and 2.45GHz LHCD system

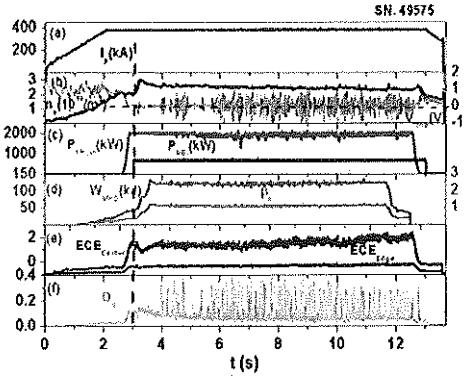

Fig. 13 Typical H-mode with 4.6GHz LHCD and NBI

Lastly, together with NBI system, repeatable H-mode plasmas are also obtained and the typical waveforms are shown in Fig. 13, in which Ip, n_e and V_{loop}, P_{LH_in} and NBI power (P_{NBI}), W_{mhd} and β_N, electron cyclotron emission in core and edge region (ECE_{Center}, ECE_{Edge}), D_a are plotted from (a) to (f). From Fig.13 (d), it is shown that the plasma energy increases to 150kJ when both the LH and NBI power are injected.

Consequently, the normalized beta reaches up to 1.2. From Figs. 13 (b) and (f), during the ELM phase, a large fluctuation in the loop voltage takes place, implying that the current drive is possibly affected by the density fluctuation in the edge region due to ELM burst. Finally, ECE measurements shown in Fig. 13 (e) indicate that the plasma emission is much stronger in the center line than that in the edge region, suggesting that wave remains mainly deposited in the core region, as in the L-mode. This is consistent with the lack of change of the loop voltage during LHCD phase and LHCD plus NBI phase .

By further comparing the D_a signal, ELM behaviors are different between the above three cases (4.6GHz alone, 4.6GHz plus 2.45GHz, and 4.6GHz plus NBI). In the H-mode with 4.6GHz, the ELMs are very small (almost ELM-free regime), possibly due to the small level of the injected power. In the case with LH at 4.6GHz and 2.45GHz, the amplitude of the ELMs is the largest (~0.9) with a frequency about 6~7 Hz. For the H-mode with LH at 4.6GHz plus NBI, the amplitude is reduced to 0.4 with an increased frequency of ~ 20Hz. The difference between the two later cases has no clear explanations yet. It may arise from different H-mode mechanisms between LHCD and neutral beam current drive (NBCD), which will be studied further later. Full time analysis of these discharges must be carried out for this purpose.

7. Conclusion and discussion

A 4.6GHz LHCD system has been firstly installed and commissioned in EAST in 2014. First LHCD results with 4.6GHz shows that LHW can be coupled to plasma with low reflection coefficient, drive plasma current and plasma rotation, modify plasma current profile, and heat plasma effectively, suggesting that it is possible to explore high performance at high density relevant to ITER.

By means of configuration optimization and local gas puffing near the LHW antenna, good LHW-plasma coupling with reflection coefficient less than 5% is obtained. The maximum LHW power coupled to plasma is up to 3.5MW.Current drive efficiency is up to $1.1\times10^{19}Am^{-2}W^{-1}$, which is a little higher than that of 2.45GHz LHW, assuming the absorption efficiency of LHW power is 75%. Plasma is simultaneously effectively heated by LHW and the central electron temperature is above 4keV, suggesting that LH power is mainly deposited in the core region. Experiments show that current profile is effectively modified, which could improve plasma confinement. Also, CD efficiency and current profile is related to launched wave spectrum, suggesting the possibility of controlling current profile by change phase difference with the system if the target plasma is enhanced further, eg., preheated by NBI or ECRH.

Repeatable H-mode plasma is obtained by either 4.6GHz LHCD system alone, or together with 2.45GHz LHCD system, NBI system. The ELM feature of H-modes is different and the related reason is under investigation.

Current drive efficiency with high density ($\sim3.7\times10^{19}m^{-3}$) in H-mode is higher than that with low density ($\sim2.7\times10^{19}m^{-3}$) in L-mode. This is possibly because CD efficiency is enhanced by less parametric instability due to the increased temperature in the edge region when the pedestal is formed. If so, CD efficiency at high density could be improved by increasing edge temperature, e.g., lithium coating

or local heating by ECRH in edge region. This could be performed in EAST later.

Acknowledgements:
This work is supported by the National Magnetic Confinement Fusion Science Program of China (Grant No. 2015GB102003, 2013GB106001, 2013GB112003), the National Natural Science Foundation of China under Grant No. 11175206, 11305211 and 11275233, and the JSPS-NRF-NSFC A3 Foresight Program in the field of Plasma Physics (NSFC No. 11261140328). It is partly supported by the China-France Collaboration program.

References:

[1] Fisch N.J. 1978 *Phys. Rev. Lett.* **41**873.
[2] Bernabei S. *et al* 1982 *Phys. Rev. Lett.* **49**1255.
[3] Fisch N.J. 1987 *Rev. Mod.Phys.* **59**175.
[4] Wan Y. X., Weng P. D., Li J. G., *et al*, "Overview progress and future plan of EAST Project" 2004 *21st International Atomic Energy Agency (IAEA) Fusion Energy Conference,* Chengdu, China, OV/1-1.
[5] Ding B. J., et al., 2013 Nucl. Fusion **55** 113027.
[6] Ding B. J. et al., 2012 *Phys. Plasma* **19** 122507.
[7] B J Ding et al., 2011 *Phys. Plasma* **18** 082510.
[8]Zhang L., et al, 2013 *Phys. Plasma***20** 062507.
[9]Kong E. H., et al., 2013*Plasma Phys. Control. Fusion* **55** 065008.
[10] Li M. H., et al., 2011 *Chin. Phys. B* **20**125202.
[11] Li M. H., et al., 2014 *Phys. Plasmas***21**062510.
[12] Moreau D.and Nguyen T. K., in Proceedings of the International Conference on Plasma Physics, Lausanne, Switzerland, June 27–July 3, 1984, Vol. 1 (1984), p. 216.
[13] Litaudon X. and Moreau D., 1990 *Nucl. Fusion***30** 471.
[14] Hillairet J. et al.,*Nucl. Fusion***50** (2010) 125010.
[15] Zang Q. et al., 2011 *Rev. Sci. Instrum.* **82** 063502.
[16] Peysson Y. and the Tore Supra Team 2001 *Nucl. Fusion* **41** 1703
[17] Decker J., et al.2014*Phys. Plasmas*, **21**, 092504
[18] Soldner F. X. et al., 1994 *Nucl. Fusion* **34** 985.
[19] Ide S. et al., 1996 *Plasma Phys. Contr. Fusion* **38** 1645.
[20] Peysson Y. et al., 2001 *Nucl. Fusion* **41** 1703.
[21] Litaudon X. et al., 2001 *Plasma Phys. Contr. Fusion* **43** 677.
[22] Ding B. J. et al., 2007 *Plasma Phys. Contr. Fusion.* **49** 563.
[23] Kuang G. L. et al., 1999 *Nucl. Fusion* **39** 1769.
[24] Wan B. N. *et al.,* 25th Fusion Energy Conference, Saint Petersburg, Russia, 13 -18 October 2014, OV/3-3
[25] Doyle E J et al., 2007 *Nucl.Fusion* **47** S18.
[26]Cesario R., et al 2010*Nature Commun.***55** 1.